UCID- 17888

Lawrence Livermore Laboratory

PERFORMANCE ANALYSIS OF AN INFRARED INTERIOR INTRUSION DETECTOR

D. R. Dunn

May, 1978

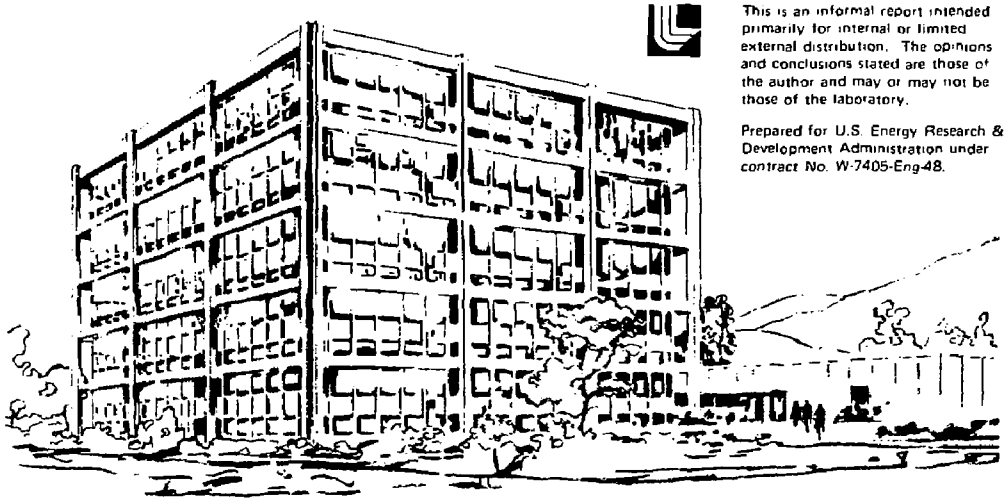

PERFORMANCE ANALYSIS OF AN INFRARED INTERIOR INTRUSION DETECTOR

by

D. R. Dunn

Lawrence Livermore Laboratory

INTRODUCTION

Component performances are required by the LLL assessment procedure for material control and accounting (MC&A) systems. See Fig. 1. Monitors are an example of an MC&A component whose functions are to process measurements or observations for purposes of detecting abnormalities.

This report develops a methodology for characterizing the performance of a class of infrared (IR) interior intrusion monitors or detectors.* The methodology is developed around a specific commercial IR detector, the InfrAlarm, manufactured by Barnes Engineering Company (Models 19-124 and 19-115A). Performance is characterized by the probability of detecting an intruder as a function of intruder parameters.

InfrAlarm is a passive infrared detector consisting of antimony and bismuth thermocouples connected to form a thermopile. IR energy emitted by objects is transmitted without physical contact to the detector receiver. The receiver in this case is a set of thermocouples which are sensitive to temperature changes.

A block diagram for the IR detector is shown in Fig. 2. The germanium lens focuses IR energy on the receiving area, physically protects the thermocouples, and segments the field of view into 10 sensitive corridors. The latter function is employed as part of the detection scheme. The lens is coated with an optical filter to remove bandwidths of light which pass through glass and hence to minimize false alarms from visible light entering through windows. The InfrAlarm's detection pattern covers a volume extending 70° horizontally and 70° vertically as shown in Fig. 3.

Each detector element senses the thermal radiation[1,2] of a small portion of the protected area. These elements, forming the pattern in Fig. 3, are connected so that energy falling within a segment produces an electrical signal. Energy impinging on adjacent segments produce signals of opposite polarities. Even if a room is nonuniform in temperature and emissivity, the

---

*This paper is a condensed version of a more detailed analysis which is to be published.

detector reaches thermal equilibrium and produces a constant output signal.

Fig. 4 idealizes the amplifier output signal occurring when an intruder crosses two adjacent segments. The InfrAlarm is designed to sense both heat and associated motion before signaling an alarm state. This feature is intended to enhance immunity to false alarming due to ambient room temperature changes, electrical interferences, and so on.

PRINCIPLE OF OPERATION

In this section we will discuss some basic equations which describe the principle of operation for an IR detector employing thermocouples.[4,6-9] A non-black body with surface area A and uniform temperature T_1 will lose heat at a rate W_s (watts) to its surroundings (assumed to be at a uniform temperature T_2) according to:

$$W_s = A\eta\,(\varepsilon(T_1)T_1^4 - \varepsilon(T_2)T_2^4)$$

where η is Stefan's constant* and $\varepsilon(T)$ is the average emissivity at temperature T. If the difference in T_1 and T_2 is small, say ΔT, then

$$W_s \approx 4A\eta\varepsilon T^3\Delta T$$

where ε is an average value. Emissivity of a material is the ratio of absorbed radiation to incident radiation. For a perfect blackbody, $\varepsilon = 1$. For metals, ε usually varies only a little over a wide range of temperature and wavelength (Ref. 7, p. 24).

The amount of power W_{in} absorbed by a detector corresponding to an IR source with intensity W_s is a function of range, R, between the detector and source, the effective aperture area, A_d, of the detector, detection pattern gain, $G(\theta,\phi)$,** optical efficiency, K_o, and detector emissivity. An expression relating these quantities is[5,7]

$$W_{in} = \frac{W_s A_d G(\theta,\phi) K_o}{\pi R^2}\,, \qquad (1)$$

*$\eta = 5.6686 \times 10^{-12}$ watt cm^{-2} $^\circ K^{-4}$

**The angles θ and ϕ represent azimuth and elevation respectively.

where the emissivity of the detector is included in the term W_s.

Absorption of radiation by a thermocouple raises the temperature of the "hot" junction relative to a "cold" junction. This temperature change will follow a thermal time constant $\tau = R_T C_T$ where R_T is the thermal resistance in °K/watt and C_T is the thermal capacitance of a thermocouple in J/°K. The temperature differential causes the detector to generate a voltage whose magnitude is a characteristic of the thermocouple material and can be related to the temperature differential by

$$\Delta V = \alpha \cdot \Delta T \qquad \text{volts},$$

where α is the thermoelectric power or Seebeck coefficient in volts/deg. The value of the Seebeck coefficient is +40 μV/°C for antimony (Sb) and -60 μV/°C for bismuth (Bi) (α = 100 μV/°C for an Sb-Bi thermocouple).

Another parameter used to characterize a thermocouple detector is responsivity, r, which normally refers to the open-circuit voltage response per incident radiation. An equation for responsivity is [7]

$$|r| = \frac{\alpha R_T}{(1 + \omega^2 \tau^2)^{1/2}} \qquad \frac{\text{volts}}{\text{watts}}$$

where ω is the frequency in radians.

The incremental voltage generated by the thermocouple array is normally amplified to produce an output voltage signal which inputs a detection circuit (see Figure 2.). Using Laplace transform notation, the output voltage signal resulting from absorption of radiation W_{in} can be expressed as:

$$V_o(s) = \frac{\alpha R_T A_v}{(s\tau + 1)(s\tau_a + 1)} W_{in}(s) \qquad (2a)$$

$$\approx \frac{r(s) A_v}{(s\tau_a + 1)} W_{in}(s) \qquad (2b)$$

where s is the complex frequency variable, A_v is the amplifier mid-frequency voltage gain, τ_a is its predominate time constant, and r(s) is responsivity.

The signal $V_o(t)$ is processed by the threshold detector and digital logic to provide a decision output regarding the presence of an

intruder. A detection model is presented following the next section which consists of a heuristic discussion on noise. The sensitivity of a thermal detector is, of course, limited by the noise in the detector system.

NOISE CONSIDERATIONS

The voltage signal appearing at the threshold element of the Infr-Alarm is contaminated by additive random noise. The noise stems from two sources: (1) electrical (viz., thermal also called Johnson noise, and shot noise) and (2) thermal fluctuations of the thermocouple elements per se. The latter case refers to temperature variations of a body due to statistical interchange of energy between the body and its surroundings.

In the former case the ohmic resistance of each thermocouple in the thermocouple array will contribute Johnson noise which has a white frequency spectrum. Furthermore, the amplifier circuitry will contribute both Johnson and shot noise.

A mathematical noise model which incorporates all of the important noise sources can be derived from knowledge of the underlying noise theory and of the circuit design. From such a model one can show that the output noise has a colored frequency spectrum, and that to compute its mean-square value and an equivalent bandwidth requires integration of the spectrum with respect to frequency. The calculations are usually lengthly and involved.

Knowledge of the output mean-squared noise voltage (σ^2) is important in characterizing the detection performance of the IR monitor. This will become apparent in the next section which shows the role that the variance parameter σ^2 plays in the detection model. For the present we will assume that σ^2 is known or can be estimated.

DETECTION MODEL

For purposes of this analysis, the output noise spectrum will be treated

as that due to zero-mean Gaussian noise with variance σ^2 over an equivalent bandwith of interest. The detection model will be based on the assumption that an intruder within any segment of the detector pattern is a constant energy source. A basic event, A_i, will be defined as a constant energy source crossing two adjacent segments of the detection pattern within a time period Δt. For a basic event to be detected, the amplifier output signal must cross both a positive and negative threshold within the time period Δt established by the digital logic.

We shall discuss the probability of detecting a basic event and the corresponding false alarm probability, conditioned upon the instrument's operating reliably. These probabilities will be denoted $P_D(BE/OP)$ and $P_{FA}(BE/OP)$, respectively, where D stands for detection, FA for false alarm, BE for basic event, and OP for operational. Probabilities that take into account the reliability of the instrument can be obtained by applying Bayes' rule. Four hypotheses have been identified for the output of the detector amplifier. Letting s represent the amplifier output signal produced by a detector target, and assuming that the time constraint is met, the hypotheses are

$H_0(\Delta t)$: Bipolar s plus noise
$H_1(\Delta t)$: Bipolar noise pulses
$H_2(\Delta t)$: Positive s plus noise
$H_3(\Delta t)$: Negative s plus noise

The theoretical probability density functions for these cases are shown in Fig. 5, where $+\delta_T$ and $-\delta_T$ represent the threshold crossing levels. The symbols $P_{D+} = P_{D-}$ and $P_{F+} = P_{F-}$ represent the corresponding shaded regions in Fig. 5.

The probability density functions for noise alone and for signal plus noise can be expressed as

$$\text{Noise:} \qquad p(y) = \frac{1}{\sqrt{2\pi}\sigma} e^{-y^2/2\sigma^2} \tag{3a}$$

$$\text{Signal + noise:} \quad p(y) = \frac{1}{\sqrt{2\pi}\sigma} e^{-(y-s)^2/2\sigma^2} \tag{3b}$$

where s is the signal parameter, σ^2 is the variance, and y is either signal or signal plus noise.

From Fig. 5 and Eqs. (3), P_{F+} and P_{D+} can be expressed as

$$P_{F+} = \int_{\delta_T/\sigma}^{\infty} \frac{1}{\sqrt{2\pi}} e^{-y^2/2}\, dy = 1-\mathrm{erf}(\delta_T/\sigma) \tag{4}$$

and

$$P_{D+} = \int_{\frac{\delta_T - s}{\sigma}}^{\infty} \frac{1}{\sqrt{2\pi}} e^{-y^2/2}\, dy = 1-\mathrm{erf}\left(\frac{\delta_T - s}{\sigma}\right) \tag{5}$$

where $\mathrm{erf}(\alpha)$ is the well known error function:

$$\mathrm{erf}(\alpha) \triangleq \frac{1}{\sqrt{2\pi}} \int_{-\infty}^{\alpha} e^{-y^2/2} dy \quad .$$

Given a set of thresholds, $\pm\delta_T$, the probability of detecting a basic event (i.e., of choosing H_o) is

$$P_D(\mathrm{BE/OP}) = P_{D+}P_{D-} = P_{D+}^2 \tag{6}$$

Inspection of Fig. 5 shows that the larger the signal $|s|$ is with repect to $|\delta_T|$ the greater the chances are for detection.

The false alarm probability is computed as

$$P_{FA}(\mathrm{BE/OP}) = 1 - (\text{Probability of no false alarm})$$
$$= 1 - (1 - P_{F+}^2)(1 - P_{D+}P_{F+})^2 \quad .$$

An intruder penetrating a detector pattern would very likely generate several basic events, thus enhancing the detection probability. The probability of detecting an intruder generating M basic events is

$$P_D(\mathrm{M/OP}) = 1 - (1 - P_{D+}^2)^M,$$

and the corresponding false alarm probability is given by

$$P_{FA}(\mathrm{M/OP}) = 1 - (1 - P_{F+}^2)^M(1 - P_{D+}P_{F+})^{2M}.$$

The performance of the InfrAlarm detector can be illustrated by receiver operating characteristic (ROC) curves that show probabilities of detection versus false alarm probabilities as a function of the target signal level.

DETECTOR PERFORMANCE

Detector performance for the InfrAlarm can be obtained from the previous analysis. We will use the parameter values from Hauffner[10] given in Table 1 below.

Table 1. Typical parameter values for analysis of InfrAlarm detector performance.

Parameter	Value	Parameter	Value
α	$100\mu V/°C$	k_0	1*
ϵ	0.95*	A_v	6.3×10^5
r_{avg}	6.33 V/W	τ_a	45.5 msec
τ	5 msec*	δ_T	1.2 V
A_d	25 cm^2*	T	300°K

*Value assumed or estimated by the author (D.R.D.)

Probability of detection curves will be shown only for basic events (i.e., M = 1) which is the conversative case.

The detection model shows that detection probability is enhanced for increasing values of amplifier output voltage or equivalently absorbed radiation due to a target. An equation for W_{in} was given in Eq. (1) and is illustrated in Fig. 6 where use was made of the values in Table 1. The thickness of the curves indicate the computed maximum and minimum variation in W_{in} due to on-axis detection and off-axis detection (see Fig. 3).

The energy emitted by a human target will vary considerably depending on the extent of exposure. A value of 50 watts is considered typical in some cases (Ref. 2, p. 5.4-1), whereas Barnes models a human target as 1 square

foot approximately 3°C above background (300°k) or about 1.7 watts[10]. Therefore, the upper shaded region in Fig. 6 could represent absorbed radiation coming from unshielded human targets. The lower shaded region, on the other hand, could represent the situation where a thermal shield of some type were employed. The 10 mw curve is for reference purposes and models a target 2 square inches in area and 1°C above backgound (about the size of a mouse).

Probability of detection curves were computed using Eqs. (2), (5), and (6) and are shown in Fig. 7 as a function of absorbed power and for two values of measurement inaccuracies. The $\sigma = 0.035$ volts is an approximation based on a noise analysis using incomplete modeling information. The $\sigma = 0.08$ volts also is an approximation but is based on typical noise levels which have been observed [10](i.e., by assuming a 3σ value equal to observed noise level). The latter value represents the more conservative case for small values of absorbed power.

The false alarm probability or equivalently false alarm rate (FAR) is established by δ_T which is nominally set at 1.2V. The result is a low value for the FAR. Comparing Figs. 6 and 7 suggests that the InfrAlarm's detection probability is excellent for a wide range of target characteristics including the case where a thermal shield might be employed.

COMPROMISING THE INFRALARM DETECTOR

In this section we examine some possible adversary acts for compromising the detector. Detector vulnerability, failure modes and reliability are all important issues, and a more comprehensive analysis would extend the ideas herein to include experimental considerations.

The InfrAlarm detector may be compromised or deceived by (1) using a thermal enclosure with an emissivity similar to the background, (2) covering the detector lens to simulate a stable background, or (3) moving into and out of dead zones, or down the axis of a detection corridor, very slowly. The first two stratagems can be countered by proper design techniques; for example, by designing the room area to have nonuniform emissivities and by including a

system self-check. The effectiveness of the third stratagem, which takes advantage of an inherent limitation of the detector, can be minimized by setting the detector pattern normal to expected pathways.

We can derive two critical velocity values for the case of constant heat flow onto the detector which relate to detector vulnerability. They are (1) the minimum velocity that an intruder running through the detector pattern must have to avoid detection, and (2) the maximum crawl velocity of an intruder for the same result. The minimum velocity is given by

$$v_{min} \triangleq \frac{\theta' R}{t_\delta}$$

where θ' is the radian width of a segment, R is the radial distance from the detector to the intruder and t_δ is the time required for $V_o(t)$ to reach the detection threshold voltage δ_T. The time t_δ can be solved from Eq. (2) for $W_{in}(t) = W$, a constant. If Eq. (2) is approximated with a single time constant (noting that $\tau_a \approx 10\tau$), the result is:

$$v_{min} = \frac{-\theta' R}{\left[\tau_a \ln\left(1 - \frac{\delta_T}{\alpha A_v R_T W}\right)\right]} . \qquad (7)$$

A plot of Eq. 7 is shown in Fig. 8 using the parameter values from Table 1. Note that the values of absorbed power W must be small (for realistic values of v_{min}) if an intruder traversing the detector pattern is to avoid crossing the detector threshold. Small values of W might possibly be achieved with a thermal shield. For example, a v_{min} of 5 m/sec at R = 5 meters corresponds to a W_{in} of 0.4 μW, and roughly corresponds to W_s = 12.6 mW and is substanially lower than that considered typical for normal human targets. Futhermore, the above results are based on an average $\epsilon(T)$. Detection probability would be enhanced if the thermal enclosure had a emissivity different from the background emissivity. It appears, therefore, that special conditions must be met before one could race across a detection pattern without being detected.

To avoid detection when crawling or walking very slowly through the detection pattern, the minimum time one can spend in any one segment or dead zone is approximately equal to Δt, the gate length of the digital logic (cf. Fig. 2). The maximum velocity is given by

$$v_{max} \triangleq \frac{\theta' R}{\Delta t} = 1.86 \times 10^{-3} R \qquad \text{m/sec}$$

where Δt = 10 seconds and a θ' = 3.5° were used. The maximum detection range for the InfraAlarm is about 15 meters and the corresponding value for v_{max} is .028m/sec, which is quite small. Even smaller rates are required for smaller values of R. Thus, traversing the detector pattern at a slow pace without being detected would probably be a difficult task.

SUMMARY AND CONCLUDING REMARKS

An analysis was undertaken to characterize the performance of a specific commercial IR detector denoted InfrAlarm. Although a lot of information with respect to detector design was available, in some instances engineering approximations were necessary. A more comprehensive analysis would necessarily involve some experimental testing. Excluded from the analysis were long term degradation and reliability considerations.

Statistical detection models for computing probabilities of detection and false alarms were derived, and the performance capability of the InfrAlarm IR detector was shown using these measures. The methodology, developed around the InfrAlarm, should be applicable to other detector designs.

The results obtained in the performance analysis show that the detection capability of the InfrAlarm is excellent (~1), with very low false alarm rates, for a wide range in target characteristics. These results should be representative and particularly for non-hostile environments.

Although several ways of compromising the detector via adversary acts were discussed, no claim on completeness is made. It was found that special conditions (viz., target cross-sectional area and temperature differential

much lower than for a typical human target) must exist for an intruder to race across the detector pattern without being detected. In addition, very low crawl velocities (<.03 m/sec) must be employed to traverse a pattern undetected.

According to Barnes[10], false alarms are normally nuisance events; that is, real infrared events due to such things as flapping papers, falling objects, or excessive rate of rise in temperature (e.g., 0.2°C/sec for a 1-foot-area space heater at a distance of 10 feet). The sensor has also been known to respond to bodies of small cross section, such as insects and mice.[2,12] A discussion of some experimental test results with respect to false alarms may be found in Ref. 2.

REFERENCES

1. Barnes, *InfrAlarm Passive Infrared Intrusion Detector Application and Installation Information* (Barnes Engineering Co., Stamford, Connecticut, circa 1977).

2. *Intrusion Detection Systems Handbook* (Sandia Laboratories, SAND 76-0554, November 1976, October 1977).

3. R. D. Hudson, Jr. and J. W. Hudson, Eds., *Infrared Detectors* (Dowden, Hutchinson, and Ross, Stroudsburg, Pennsylvania, 1975).

4. E. H. Putley, "Modern Infrared Detectors." Reprinted in Reference 3, p. 30.

5. Dianne Earing, "Thin Film Thermopile Detectors and Their Commercial Application," *Proc. Society of Photo-Optical Instrumentation Engineers*, vol. 62, p. 60 (1975).

6. E. H. Putley, "Solid State Devices for Infra-Red Detection." Reprinted in Reference 3, p. 18.

7. R. A. Smith et al., *The Detection and Measurement of Infra-Red Radiation* (Oxford University Press, New York, 1968).

8. J. A. Jamieson et al., *Infrared Physics and Engineering* (McGraw-Hill, New York, 1963).

9. N. B. Stevens, "Radiation Thermopiles," Chapter 7 of *Semiconductors and Semimetals* vol. V (Infrared Detectors), R. K. Willardson and A. C. Beer, Eds. (Academic Press, New York, 1970).

10. S. Hauffner, Barnes Engineering Co., Stamford, Connecticut, private communications (August-October, 1977).

11. *Fairchild Linear Integrated Circuits Catalog* (February, 1973).

12. D. Mangun, Sandia Laboratories, Albuquerque, New Mexico, private communication (August-October, 1977).

This report was prepared as an account of work sponsored by the U.S. Nuclear Regulatory Commission, under the auspices of the U.S. Department of Energy Contract No. W-7405-ENG-48.

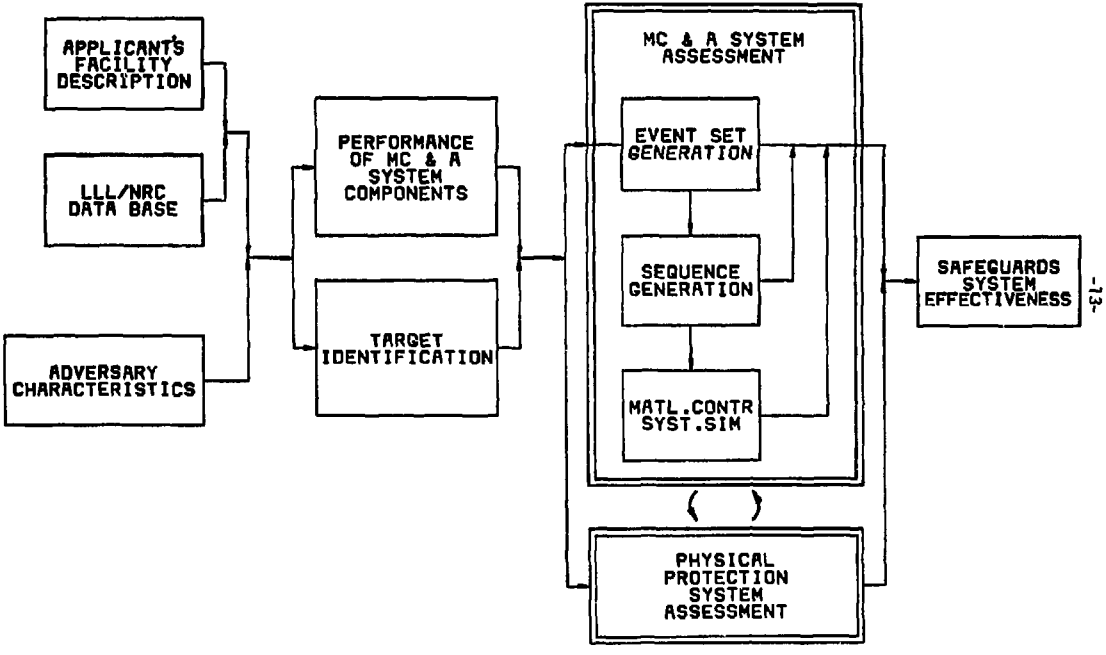

Fig. 1 The LLL Assessment Procedure

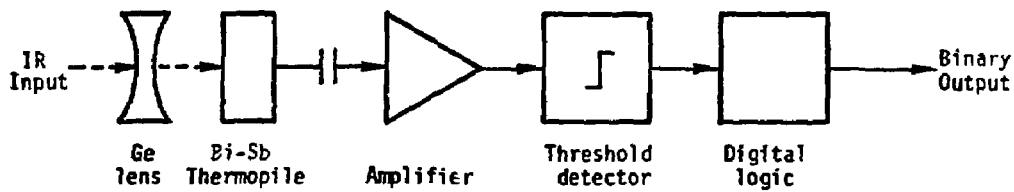

Fig. 2. Block diagram of IR detector.

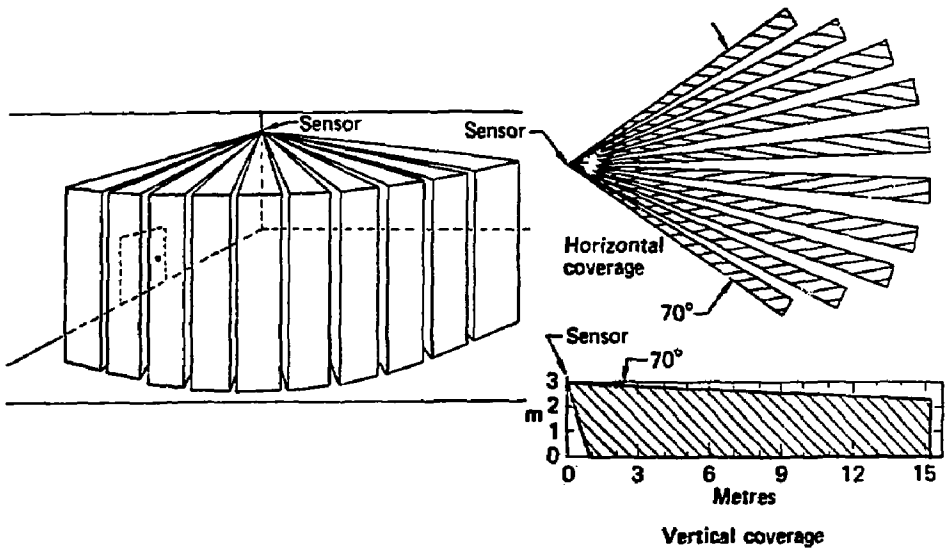

Fig. 3. Typical Barnes InfrAlarm detection pattern.

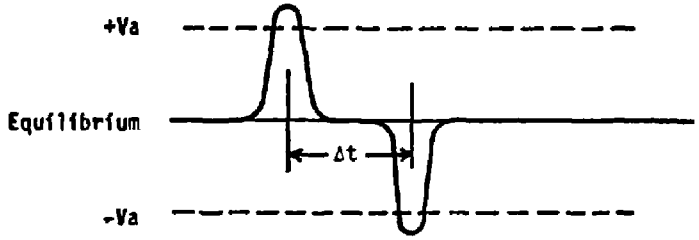

Fig. 4. Idealized output signal of amplifier.

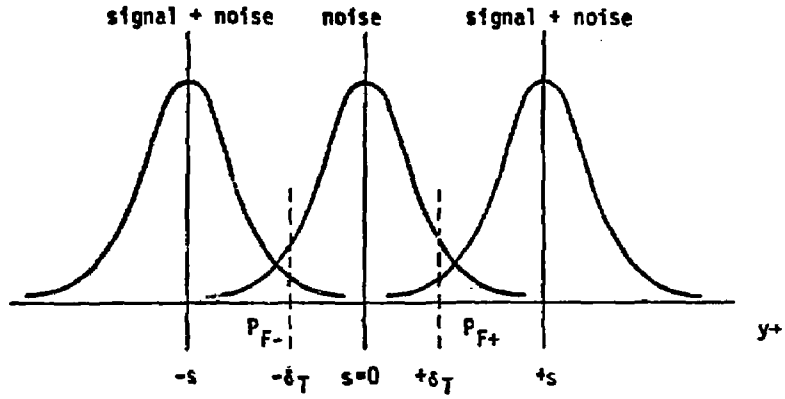

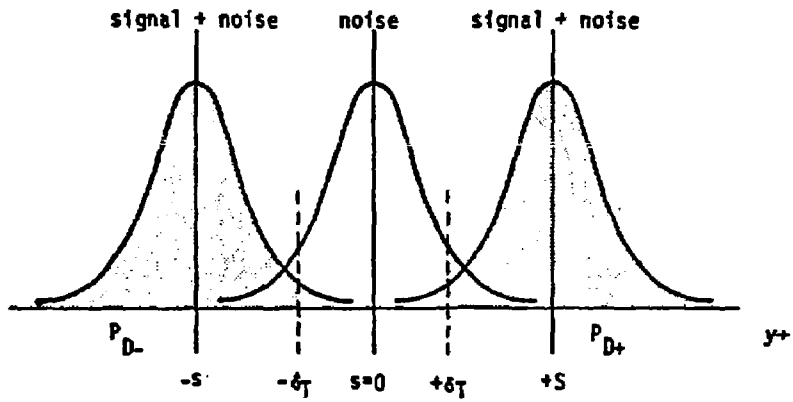

Fig. 5. Theoretical probability density functions for signal and noise.

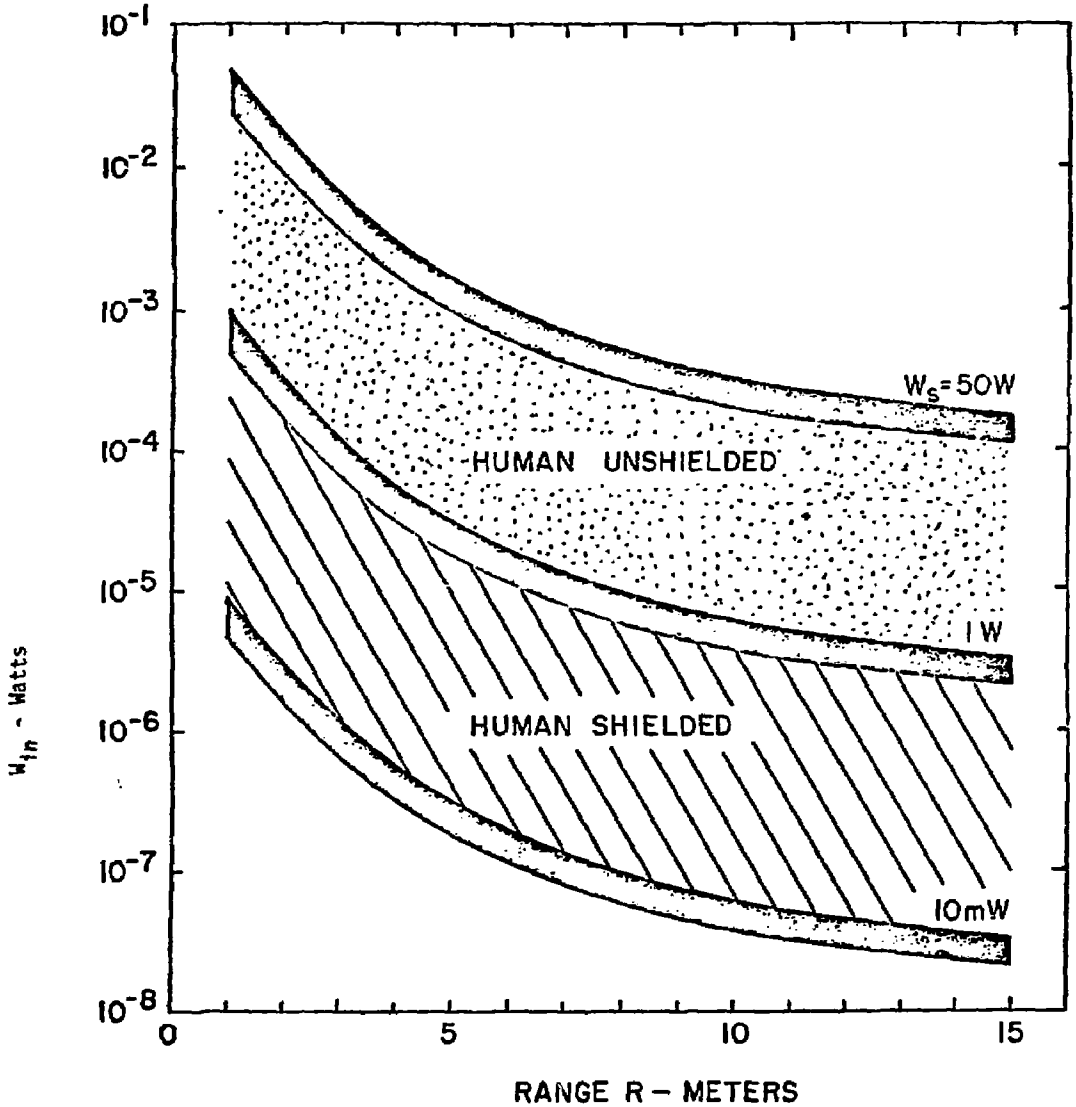

Fig. 6 Absorbed Power, W_{in}, as a Function of R and Ws

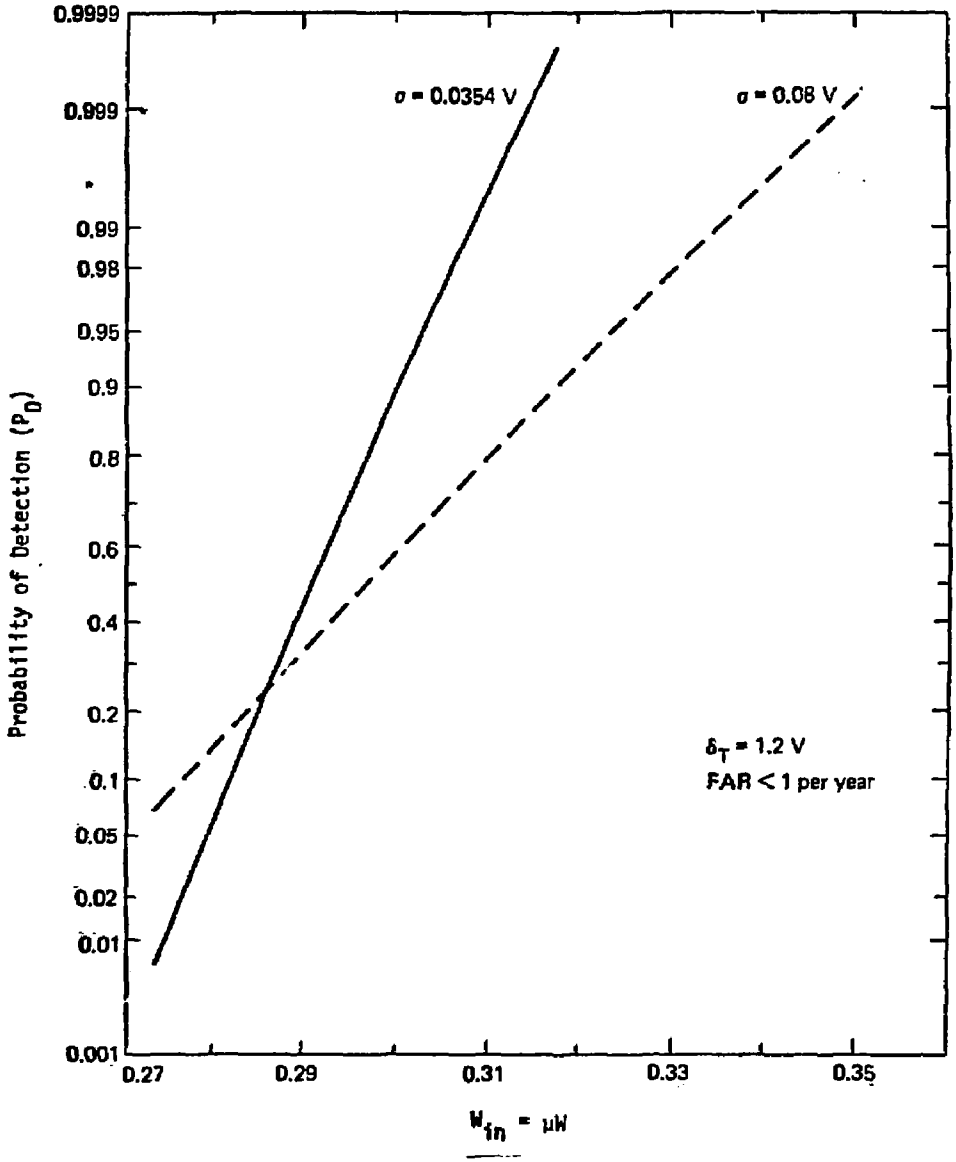

Fig. 7. Probability of detection versus absorbed power W_{in}.

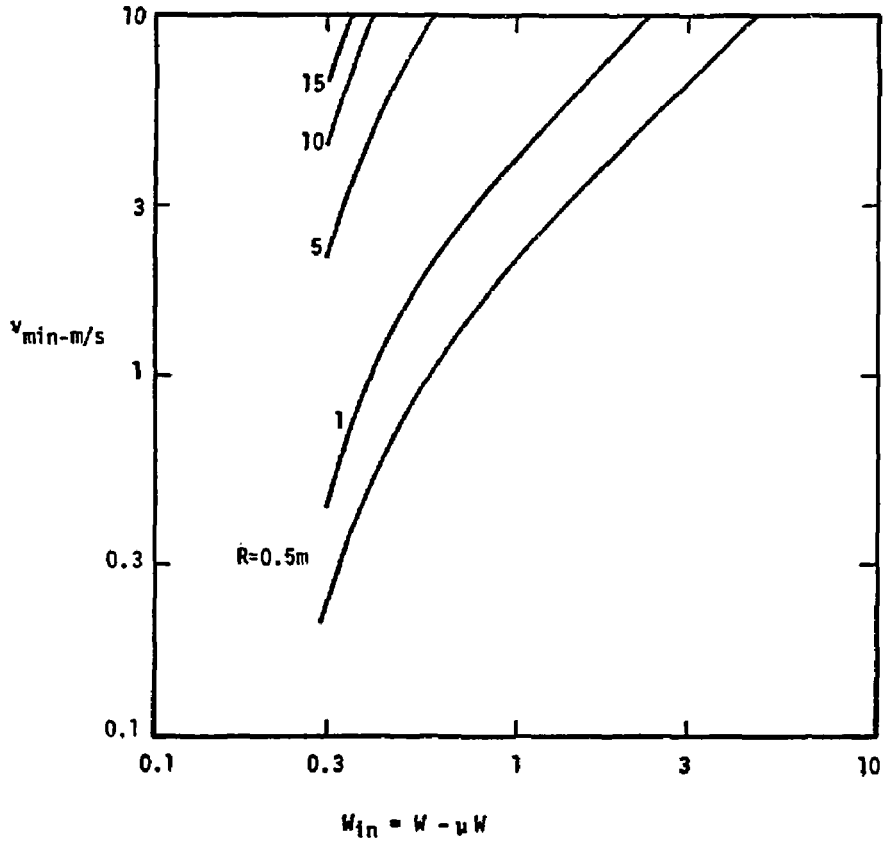

Fig. 8. Velocity v_{min} as a function of W_{in} and R.